A Computational Study of the Thermal Cycloreversion of 2,2,6-Trimethyl-4*H*-1,3-dioxin-4-one and a Related Species: Retro-Diels–Alder Reaction or Concerted Nucleophilic Attack?

Shawn W. E. Eisenberg, Mark J. Kurth,† and William H. Fink*

Department of Chemistry, University of California, Davis, California 95616

Received March 9, 1995®

Calculations up to the MP2/6-31G*//HF/3-21G level have been carried out to study the thermal cycloreversion of 2,2,6-trimethyl-4*H*-1,3-dioxin-4-one (**1**) and 2,2,4-trimethyl-6*H*-1,3-oxazin-6-one (**3**). At this level of calculation, the enthalpy of activation for the thermal cycloreversion of dioxinone **1** was found to be 31.3 kcal/mol with zero-point vibrational energy correction. The experimental value for the reaction in solution is 30.4 kcal/mol. The enthalpy of activation for the as of yet unsynthesized oxazinone **3** was found to be 44.2 kcal/mol with zero-point correction. Contrasting with the standard view that the thermal cycloreversion of dioxinone **1** is a retro-Diels–Alder reaction is the structural information from the HF/3-21G-optimized transition state **5** which shows the plane of the acetone dienophile tilted roughly 90° to the plane of the acylketene diene.

Introduction

The use of commercially available 2,2,6-trimethyl-4*H*-1,3-dioxin-4-one (**1**) for a variety of synthetic purposes is becoming widespread. Known as the "diketene–acetone adduct", dioxinone **1** undergoes thermal cycloreversion to yield acetone and acylketene at synthetically useful rates when heated above 100 °C. The acylketene can then be trapped by a variety of nucleophiles. In this capacity, dioxinones have been used to form β-keto esters,[1] thioesters,[1] amides,[2] lactones,[3] and lactams.[4] Other synthetic applications using dioxinones include [2 + 2] photoadditions[5] and Michael[6] additions to the 4*H*-1,3-dioxin-4-one system, as well as other additions[7] to dioxinone-generated acylketenes.

Work in our lab on dioxinone-mediated cyclizations has led to some interesting observations (see Scheme 1). When the cyclization precursor is heated in refluxing toluene, none of the expected 11-membered lactone is formed. Instead, the dimeric (22-membered ring), trimeric (33-membered ring),[8] and higher order macrolides are produced.[9] Our difficulties in cyclizing to the 11-membered ring, combined with our ongoing studies of polymer-supported synthetic methodology,[10] sparked our interest in finding a dioxinone analog which could be tethered to a polymer support. In particular, we were

Scheme 1

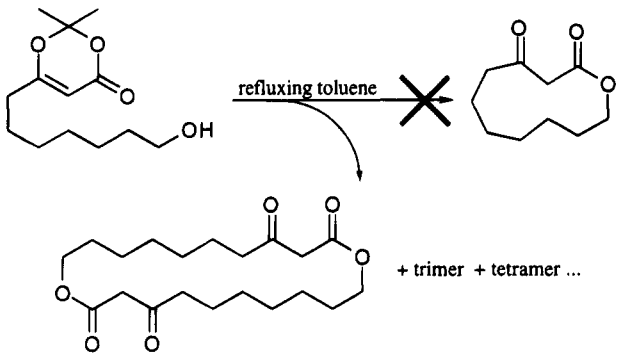

Scheme 2

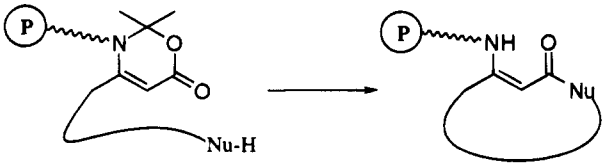

intrigued by the possibility that 2,2,4-trimethyl-6*H*-1,3-oxazin-6-one (**3**) might undergo a thermal cycloreversion similar to that of dioxinone **1** (see eqs 1 and 2).

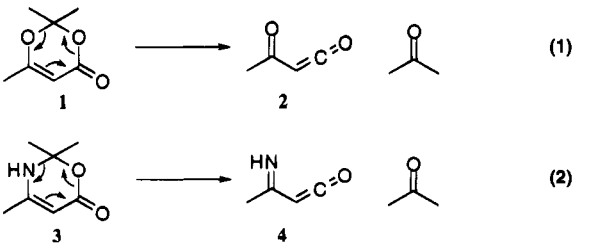

The potential synthetic utility of this is shown in Scheme 2, where oxazinone **3** is site-isolated by linking its amino moiety to a polymer support. This should

† Author to whom synthetic inquiries should be addressed.
® Abstract published in *Advance ACS Abstracts,* May 15, 1995.

(1) Clemens, R. J.; Hyatt, J. A. *J. Org. Chem.* **1985**, *50*, 2431.
(2) (a) Jones, R. C. F.; Tankard, M. *J. Chem. Soc., Perkin Trans. 1* **1990**, 240. (b) Avendano, C.; de la Cuesta, E.; Gesto, C. *Synthesis* **1991**, 727. (c) Boeckman, R. K., Jr.; Thomas, A. J. *J. Org. Chem.* **1982**, *47*, 2823. (d) Sato, M.; Kanuwa, N.; Kato, T. *Chem. Pharm. Bull.* **1982**, *30*, 1315.
(3) (a) Petasis, N. A.; Pantane, M. A. *J. Chem. Soc., Chem. Commun.* **1990**, 836. (b) Boeckman, R. K., Jr.; Pruitt, J. R. *J. Am. Chem. Soc.* **1989**, *111*, 8286. (c) Sato, M.; Sakaki, J.; Takayama, K.; Kobayashi, S.; Suzuki, M.; Kaneko, C. *Chem. Pharm. Bull.* **1990**, *38*, 94.
(4) Boeckman, R. K., Jr.; Perni, R. B. *J. Org. Chem.* **1986**, *51*, 5486.
(5) (a) Lange, L. G.; Organ, M. G. *Tetrahedron Lett.* **1993**, *34*, 1425. (b) Demuth, M.; Palomer, A. *Angew. Chem., Int. Ed. Engl.* **1986**, *25*, 1117. (c) Seeback, D.; Zimmermann, J. *Helv. Chim. Acta* **1986**, *69*, 1147.
(6) Seeback, D.; Zimmermann, J.; Gysel, M.; Ziegler, R.; Ha, T. K. *J. Am. Chem. Soc.* **1988**, *110*, 4763.
(7) Coleman, R. S.; Fraser, J. R. *J. Org. Chem.* **1993**, *58*, 385.
(8) Chen, C.; Quin, E. K.; Olmstead, M. M.; Kurth, M. J. *J. Org. Chem.* **1993**, *58*, 5011.
(9) Eisenberg, S. W. E.; Chen, C.; Wu, J.; Jones, A. D.; Fink, W. H.; Lebrilla, C. B.; Kurth, M. J. Unpublished results.
(10) (a) Moon, H. S.; Schore, N. E.; Kurth, M. J. *J. Org. Chem.* **1992**, *57*, 6088. (b) Beebe, X.; Schore, N. E.; Kurth, M. J. *J. Am. Chem. Soc.* **1992**, *114*, 10061. (c) Chen, C.; Alberg Randall, L. A.; Miller, R. B.; Jones, A. D.; Kurth, M. J. *J. Am. Chem. Soc.* **1994**, *116*, 2661. For excellent reviews, see: (d) Jung, G.; Beck-Sickinger, A. G. *Angew. Chem., Int. Ed. Engl.* **1992**, *31*, 367. (e) Pavia, M. R.; Sawyer, T. K.; Moos, W. H. *Bioorg. Med. Chem. Lett.* **1993**, *3*, 387.

0022-3263/95/1960-3736$09.00/0 © 1995 American Chemical Society

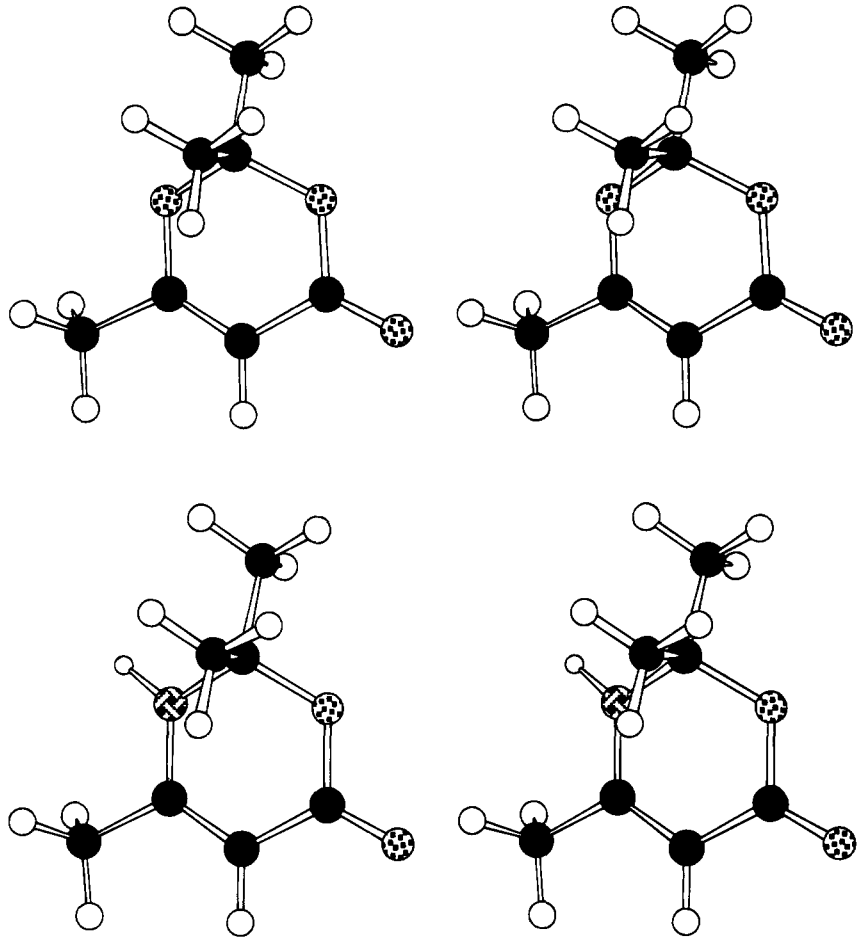

Figure 1. Stereoviews of HF/3-21G-optimized geometries for dioxinone **1**, top, and oxazinone **3**, bottom.

facilitate lactone and lactone analog cyclization without the need for high dilution, a requirement in dioxinone-mediated cyclizations. This idea prompted us to pursue the transition state geometries for the thermal cycloreversion of dioxinone **1** and oxazinone **3**. By comparing theoretical energies of activation for dioxinone **1** and oxazinone **3**, we hoped to judge whether oxazinone **3** would undergo thermal decomposition at temperatures similar to those required for dioxinone **1**.

Wishing for a benchmark by which to calibrate our calculations, we found it necessary to have access to experimental data. This was elegantly supplied in a series of kinetic and spectroscopic studies[11] by Witzeman and Clemens in which they studied the thermal decomposition of dioxinone **1** under a variety of conditions with various trapping nucleophiles. They have shown that dioxinone **1** undergoes thermal cycloreversion at temperatures above 80 °C to yield acetone and acylketene. The acylketene, though often postulated for this process,[1,12] had never been isolated as an intermediate in this reaction until Witzeman and Clemens observed it by FT-IR (trapped in an argon matrix). With a variety of chemical reaction probes, they concluded that this was a concerted process, likely a retro-Diels–Alder reaction. The MINDO/3 intrinsic reaction coordinate study of the dioxinone **1** system by Hong and Fu[13] is in agreement with this view of the thermal elimination.

In this paper, we report calculated energies which show that thermal cycloreversion is more fascile for dioxinone **1** than for oxazinone **3**. Additionally, we present qualitative structural details concerning the transition state geometries for the thermal cycloreversion of dioxinone **1** and oxazinone **3**. We also show how these details bear on the accepted view that the thermal cycloreversion of dioxinone **1** is a retro-Diels–Alder process. This is illustrated later by comparing transition states **5** and **6** with that for the prototypical Diels–Alder reaction between ethene and butadiene.

Results

All structures were optimized using Spartan[14] software. Initial starting guess geometries were generated using Biosym's Insight II Builder[15] module. All[16] transition states were subjected to force analysis and were verified as having only one imaginary frequency corresponding to the expected bond breaking or making.

(11) Clemens, R. J.; Witzeman, J. S. *J. Am. Chem. Soc.* **1989**, *111*, 2186.

(12) Sato, M.; Ogasawara, H.; Oi, K.; Kato, T. *Chem. Pharm. Bull.* **1983**, *31*, 1896.

(13) Hong, S. G.; Fu, X. Y. *THEOCHEM* **1990**, *209*, 241. Though not mentioned, from the structural data given in this paper, it appears that the dioxinone reactant and transition state were optimized making the assumption that there is a mirror plane of symmetry running through the molecule. This constrains the ring systems in the transition state and the reactant to planar geometries. Our calculations do not make this constraint, and consequently, we do not come to the same structural conclusions as Hong and Fu.

(14) *Spartan*, Version 3.0.1; Wavefunction Inc., 18401 Von Karman Suite 370: Irvine, CA 92715, 1991–1993.

(15) *InsightII*, Version 3.2.0; Biosym Technologies Inc., 9685 Scranton Road: San Diego, CA 92121-2777.

(16) Excepting the 4*H*-1,3-dioxin-4-one model study mentioned later in this paper.

Chart 1

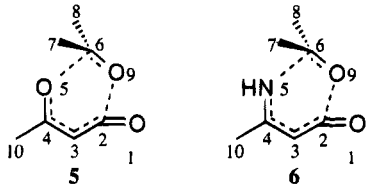

5 **6**

Table 1. Electronic Energy Data for the Optimized Structures

structure	AM1[a]	HF/3-21G[b]	HF/6-31G*// HF/3-21G[b]	MP2/6-31G*// HF/3-21G[b]
dioxinone **1**	−113.5	−492.747 99	−495.498 56	−496.922 62
oxazinone **3**	−69.5	−473.026 18	−475.665 63	−477.077 60
acylketene **2**	−48.2	−301.801 43	−303.502 19	−304.352 43
iminyl ketene **4**	4.0	−282.060 52	−283.652 24	−284.488 25
acetone	−49.2	−190.887 22	−191.961 39	−192.523 05
TS **5**[c]	−83.0	−492.680 73	−495.434 69	−496.867 15
TS **6**[c]	−22.7	−472.935 33	−475.583 14	−477.001 64

[a] Kilocalories per mole. [b] Hartrees. [c] Transition state geometry (TS).

Additionally, all HF/STO-3G- and HF/3-21G-optimized structures were subjected to force analysis to supply zero-point vibrational energy data and to confirm that the minima had no imaginary frequencies. Electronic energy results are provided in Table 1.

Transition state **5** was first located by modifying an AM1 ethene−butadiene Diels−Alder transition state by appropriate substitution of carbons and hydrogens with oxygens and methyl groups. These modifications consisted of replacement with one or two atoms or methyl groups at a time with reoptimization between each change and frequency analysis to affirm that stationary points were indeed transition states. This procedure led to a structure not shown but similar to that depicted in Figure 2. Following the intrinsic reaction coordinate in either direction leads to starting material or products, as expected.

As is evident, this structure has deviated significantly from its origins (see Figure 4). Using the numbering scheme outlined in schematic transition state **5**, one notices that O9, C6, C7, and C8 make up the leaving acetone moiety. The remainder of the heavy atoms make up the forming acylketene. The breaking bonds, O9−C2 (1.547 Å) and O5−C6 (2.213 Å), show a highly asymmetric concerted process. These bond lengths should be compared with the optimized AM1 dioxinone **1** values of O9−C2 (1.228 Å) and O5−C6 (1.441 Å). The forming acetone carbonyl π-bond is already quite well-developed at 1.289 Å in the transition state. Starting from this transition state, we reoptimized this structure using the STO-3G basis set at a Hartree−Fock level of calculation, but as expected, the relative energies of the HF/STO-3G-optimized structures were in poor agreement with the experimentally determined activation energy.

Since the size of dioxinone **1** is somewhat daunting even for present high-speed workstations, a model study[17] was undertaken to ascertain the minimum basis set complexity that would be reliable. We examined the transition state structure of 4*H*-1,3-dioxin-4-one (dioxinone **1** minus the three pendant methyl groups) with the STO-3G, 3-21G, and 6-31G* basis sets. The HF/6-31G*-optimized structure was in good agreement with the HF/3-21G structure but much less so with the HF/STO-3G structure.[18] We took this agreement to suggest that the optimized structures from the HF/3-21G calculations would be adequate for use in single-point calculations at more sophisticated levels for determining relative energies of dioxinone **1** and oxazinone **3**.

The HF/3-21G-optimized transition state is shown in Figure 2. In these stereoviews of the transition state structures, the shaded bonds represent the breaking bonds. Consistent with concerted bond making and bond breaking, O9−C2 (1.868 Å) and O5−C6 (2.116 Å) are both quite extended and the forming acetone carbonyl bond is already foreshortened at 1.249 Å. As can be seen in Table 2, the bond length changes in going from dioxinone **1** to transition state **5** correspond to the formation of new double bonds at C4−O5, the forming β-keto group, and at C2−C3, the forming ketene carbon−carbon double bond. The Mulliken bond orders shown in Table 3 reflect these changes with bond orders of 1.56 for C4−O5, 1.28 for C2−C3, and 1.05 for the nascent single bond between C3 and C4. These bond orders can be compared with those for HF/3-21G-optimized dioxinone **1**: C4−O5 (0.89), C2−C3 (0.97), and C3−C4 (1.59). Expected but worth noting is the observation that the forming ketene carbonyl, O1−C2, appears almost completely divorced from this process, retaining essential double bond character throughout, with a Mulliken bond order of 1.78 in dioxinone **1** and 1.92 in transition state **5**.

Bond angles in the HF/3-21G-optimized transition state mirror what is evident from bond lengths and orders. The acylketene itself is partially formed with a C3−C2−O1 bond angle of 150.9° as compared with 126.0° for HF/3-21G-optimized dioxinone **1**. The acetone carbonyl carbon, C6, appears almost completely rehybridized, showing bond angles of 122.2° for C7−C6−O9, 116.3° for C7−C6−C8, and 119.7° for C8−C6−O9 as opposed to 110.0° for C7−C6−O9, 114.1° for C7−C6−C8, and 107.2° for C8−C6−O9 for dioxinone **1**. A comparison of the bond angles for acetone optimized with the 3-21G basis set, C−C−C (115.0°) and C−C−O (122.5°), shows that the bond angles for the acetone moiety in the transition state are similar to those for the equilibrium geometry of acetone.

Turning now to the overall geometry of the transition state shown in Figure 2, the dioxinone transition state is asymmetric as is common for heterocyclic transition states.[19] Additionally, the cyclic transition state takes an envelope form where the acylketene moiety and the acetone carbonyl carbon form the planar portion of the envelope with the carbonyl oxygen of the acetone moiety acting as the open flap, thus being slightly out of the plane. The plane of the acetone is tilted nearly 90° with respect to the plane of the acylketene, placing the acetone's methyl groups both above and below the plane of the acylketene. The orientation of these methyl groups

(17) We thank a reviewer for suggesting this model study.

(18) The average difference in bond lengths between the HF/STO-3G and the HF/6-31G* structures is 0.0311 Å, and the average difference in bond lengths between the HF/3-21G- and the HF/6-31G*-optimized structures is 0.0188 Å. With the exception of one bond (C2−C3), all the HF/6-31G* bond lengths were consistently shorter than those in the HF/STO-3G-optimized structure. In the HF/3-21G-optimized structure, there were a mix of bonds which were longer and shorter than those in the HF/6-31G*-optimized transition state.

(19) Hetero-Diels−Alder: (a) Mc Carrick, M. A.; Yun-Dong, W.; Houk, K. N. *J. Org. Chem.* **1993**, *58*, 3330. (b) Conzalez, J.; Taylor, E. C.; Houk, K. N. *J. Org. Chem.* **1992**, *57*, 3753. (c) Singleton, D. A. *J. Am. Chem. Soc.* **1992**, *114*, 6563. A loose analogy can be drawn in the heteroene reaction: (d) Thomas, B. E.; Houk, K. N. *J. Am. Chem. Soc.* **1993**, *115*, 790.

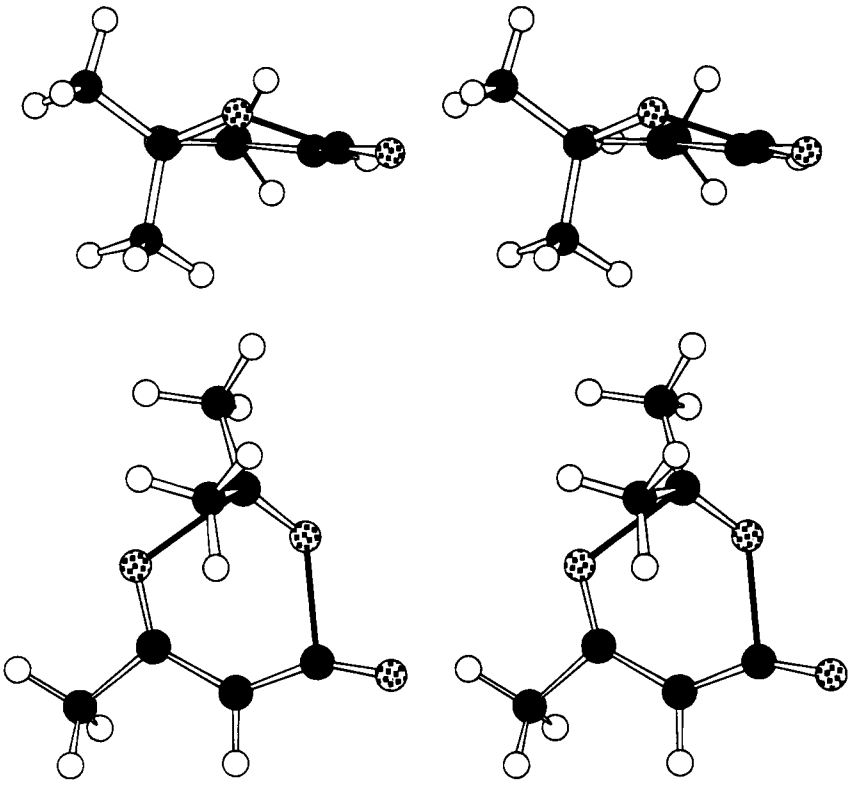

Figure 2. Stereoviews of the HF/3-21G-optimized transition state for the thermal cycloreversion of dioxinone **2**.

Table 2. Selected Bond Lengths, Angles, and Dihedral Angles[a]

atoms	dioxinone **1**	TS **5**[c]	oxazinone **3**	TS **6**[c]
		Bond Lengths[b]		
1,2	1.198	1.161	1.201	1.157
2,3	1.458	1.353	1.452	1.335
3,4	1.325	1.422	1.339	1.442
4,5	1.364	1.242	1.361	1.271
5,6	1.450	2.116	1.461	2.127
6,9	1.431	1.249	1.440	1.245
9,2	1.381	1.868	1.385	2.034
		Bond Angles[b]		
1,2,3	126.0	150.9	126.2	156.9
2,3,4	121.0	131.7	121.0	134.0
5,6,9	110.0	96.4	109.1	98.1
8,6,9	107.2	119.7	105.9	119.7
		Dihedral Angles[b]		
2,3,4,5	−5.6	−8.2	−9.5	−8.9
3,4,5,6	−15.4	2.1	−11.1	8.2
3,2,9,6	23.8	49.1	25.8	48.0
9,2,3,4	1.9	8.5	2.5	−11.0

[a] Table entries are for structures optimized at the HF/3-21G level. [b] Bond lengths are in units of angstroms; bond angles and dihedral angles are in units of degrees. [c] Transition state geometry (TS).

in the transition state reflects their orientation in the reactant, dioxinone **1** (Figure 1).

Examining the enthalpy of activation (Table 4), one notes that the computationally inexpensive AM1-calculated $\Delta H^{\ddagger} = 30.5$ kcal/mol is in closest agreement with the kinetically measured[11] value of $\Delta H^{\ddagger} = 30.4$ kcal/mol. The enthalpy of activation for the HF/3-21G-optimized structures is $\Delta H^{\ddagger} = 38.7$ kcal/mol. Single-point calculations using the higher basis set 6-31G* give HF/6-31G*//HF/3-21G (ZPE) $\Delta H^{\ddagger} = 36.5$ kcal/mol. Incorporating electron correlation lowers the value to MP2/6-31G*//HF/3-21G (ZPE) $\Delta H^{\ddagger} = 31.3$ kcal/mol. All three of these calculations are in moderate agreement with each other.

Table 3. Selected Mulliken Bond Orders for HF/3-21G-Optimized Structures[a]

	bond order				
compound	1,2	2,3	3,4	4,5	6,9
dioxinone **1**	1.78	0.97	1.59	0.89	0.80
TS **5**	1.92	1.28	1.05	1.56	1.44
oxazinone **3**	1.76	0.99	1.54	0.91	0.81
TS **6**	1.95	1.38	1.03	1.61	1.51
acetone	–	–	–	–	1.86
acylketene **2**	2.04	1.47	0.91	1.81	–
iminyl ketene **4**	2.02	1.51	0.96	1.83	–

[a] The atom-numbering scheme can be found in the schematic representation and numbering scheme outlined previously in this paper. Numbering for the product structures is assigned as if they were still part of schematic transition states **5** and **6**; e.g. acetone carbonyl carbon is C6. Bond orders are in units of bonds.

Though these numbers are gratifyingly close to the kinetically measured energy of activation, it should be pointed out that semiempirical calculations and small basis set *ab initio* calculations should be treated as qualitative rather than quantitative models. Further, the experimental value is from a solution phase reaction, whereas the calculations are for gas phase species. Therefore, one should keep in mind that there is an element of serendipity associated with the accuracy of these values.

Having examined energetic data using a range of computational tools, we turned to an examination of the transition state geometry for the thermal cycloreversion of oxazinone **3**, the original reason we undertook these calculations. The AM1 transition state for the thermal cycloreversion of oxazinone **3** was located by replacing O5 on the AM1 dioxinone transition state with an NH. This was then optimized to a saddle point. This AM1 transition state is qualitatively similar to that shown in Figure 3. The AM1-optimized transition state has the expected extended bonds: O9−C2 (1.518 Å) and N5−C6

Table 4. Calculated Relative Energies (kcal/mol)

calculation level	E_a (eq 1)	E_a (eq 2)	E_a (eq 1 (r))[a]	E_a (eq 2 (r))[a]	E_{rxn} (eq 1)[b]	E_{rxn} (eq 2)[b]
AM1	30.5	46.8	14.5	22.5	16.1	24.2
HF/STO-3G	92.6	96.6	13.3	14.7	79.3	81.9
HF/STO-3G (ZPE)[c]	88.5	92.3	14.7	16.1	73.8	76.3
HF/6-31G*//HF/STO-3G	36.1	49.7	16.6	19.6	19.5	30.1
HF/6-31G*//HF/STO-3G (ZPE)[c]	32.0	45.4	17.9	21.0	14.1	24.4
MP2/6-31G*//HF/STO-3G	33.4	47.0	5.3	3.0	28.1	38.5
MP2/6-31G*//HF/STO-3G (ZPE)[c]	29.3	41.8	6.7	4.4	22.6	32.8
HF/3-21G	42.2	57.0	5.0	7.8	37.2	49.2
HF/3-21G (ZPE)[c]	38.7	53.5	6.6	9.2	32.0	44.0
HF/6-31G*//HF/3-21G	40.1	51.8	18.1	19.1	22.0	32.6
HF/6-31G*//HF/3-21G (ZPE)[c]	36.5	48.2	19.8	20.9	16.7	27.4
MP2/6-31G*//HF/3-21G	34.8	47.7	5.2	6.1	29.6	41.6
MP2/6-31G*//HF/3-21G (ZPE)[c]	31.3	44.2	6.9	7.8	24.4	36.3

[a] Energy of activation for the reverse reaction. [b] Energy of reaction. [c] Zero-point energy-corrected values. Zero-point energies taken from vibrational analyses at the basis set used for the optimization.

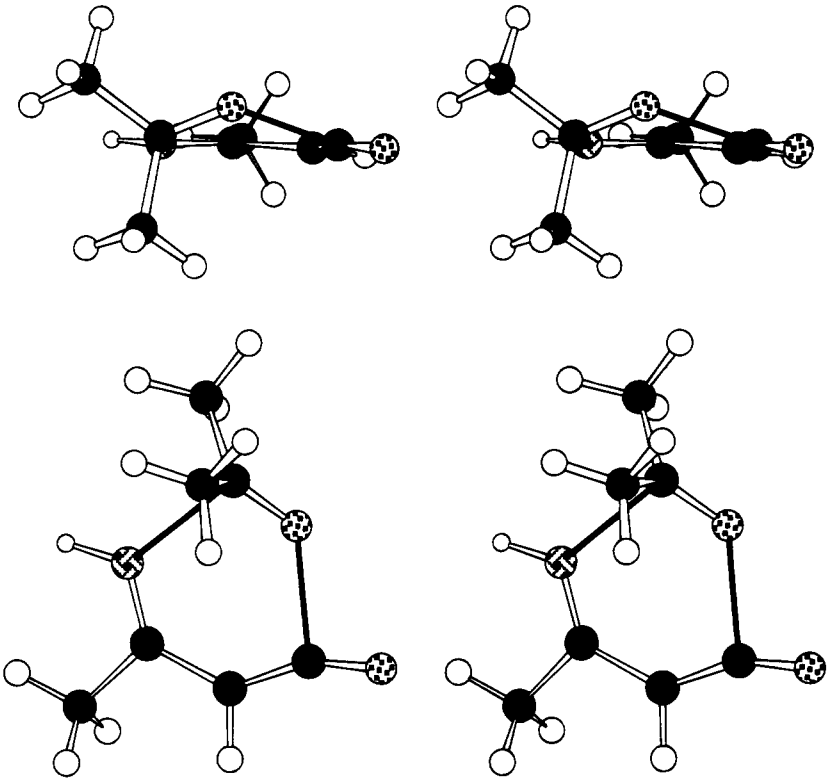

Figure 3. Stereoviews of the HF/3-21G-optimized transition state for the thermal cycloreversion of oxazinone **3**.

(2.191 Å). These bond lengths can be compared to their counterparts in the AM1-optimized oxazinone: O9–C2 (1.384 Å) and N5–C6 (1.465 Å).

The AM1 transition state was reoptimized using the STO-3G basis set and again reoptimized using the 3-21G basis set for aforementioned reasons to give the structure shown in Figure 3. The HF/3-21G-optimized structure shows the breaking bonds at O9–C2 (2.034 Å) and N5–C6 (2.127 Å). Reviewing Table 2, one notes that, in analogy to dioxinone transition state **5**, key bonds are lengthening and contracting in oxazinone transition state **6**. Specifically, the C2–C3, C4–N5, and C6–O9 bonds are shortening to form the iminyl ketene and acetone π-bonds. The bond lengths and Mulliken bond orders (see Table 3) show that the C3–C4 double bond (1.339 Å, bond order 1.54) in oxazinone has, in the transition state (1.442 Å, 1.03), progressed well toward the single bond (1.469 Å, 0.96) of the HF/3-21G-optimized iminyl ketene **4** product. The C6–O9 bond length and order (1.245 Å, 1.51) in the transition state show that the carbonyl of the acetone moiety is well-formed in this system, compared with the carbonyl in the HF/3-21G-optimized acetone (1.211 Å, 1.86).

Paralleling dioxinone transition state **5**, the acetone moiety's bond angles in oxazinone transition state **6**, C7–C6–O9 (121.4°), C7–C6–C8 (115.4°), and C8–C6–O9 (119.7°), show evidence of rehybridization of the sp^3-hybridized center in oxazinone **3** to the sp^2-hybridized center of acetone. As a means of calibrating the bond angle changes in the transition state, the analogous bond angles for oxazinone **3** are provided: C7–C6–O9 (108.7°), C7–C6–C8 (112.4°), and C8–C6–O9 (105.9°). As is evident from Figure 3, the nascent ketene is in the process of linearizing in the transition state with a O1–C2–C3 bond angle of 156.9°, compared with a bond angle of 126.2° in the HF/3-21G-optimized oxazinone. The gross structural features of transition state **6** are quite similar to those of transition state **5**. The acetone is leaving from in the plane of the ketene, with the plane of the acetone moiety tilted roughly 90° from the plane of the iminyl ketene moiety. The bond breaking is asymmetric with a longer N5–C6 bond. The overall

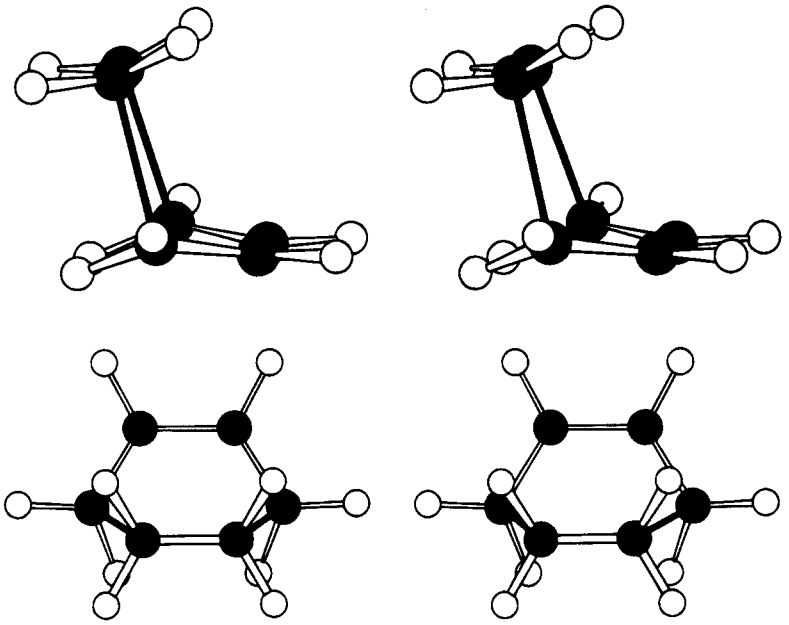

Figure 4. Stereoviews of the AM1-optimized transition state for the Diels–Alder reaction between ethene and butadiene. This view is provided to show a qualitative picture of a Diels–Alder transition state for the purpose of visual, comparison with other transition states presented in this paper.

appearance of this transition state still bears resemblance to the HF/3-21G-optimized oxazinone **3** (Figure 1).

The predicted enthalpy of activation for the thermal cycloreversion of oxazinone **3** using the AM1 Hamiltonian is 46.8 kcal/mol. Since no experimental data are available for this compound, the best that can be done is to compare values at different levels of theory. In the ZPE-corrected enthalpy of activation values shown in Table 4, it is evident that the HF/6-31G*//HF/STO-3G (ZPE) $\Delta H^{\ddagger}$ = 45.4 kcal/mol and HF/6-31G*//HF/3-21G (ZPE) $\Delta H^{\ddagger}$ = 48.2 kcal/mol activation energies are in closest agreement with the AM1 value; though generally all the 6-31G* single-point calculations as well as the HF/3-21G calculation are in relatively close agreement with each other.

Discussion

Comparing Figures 2 and 4 shows the striking differences between the transition state for the prototypical Diels–Alder reaction between ethene and butadiene and transition state **5** for the reaction between the acetone dienophile and the acyl ketene diene. The symmetry of the Diels–Alder transition state contrasting with the asymmetry of the dioxinone transition state **5** is visually striking but not surprising due to the heterocyclic nature of the dioxinone system. Hetero-Diels–Alder reactions also tend to have asymmetric bond making/breaking in the transition state to the point at which the transition state can be quite distinct[19] from the ethene–butadiene transition state. What drives a wedge between the Diels–Alder transition state and transition state **5** is the attack angle on the dienophile. In the Diels–Alder transition state shown in Figure 4, the ethene approaches butadiene from an angle slightly larger than 90°. In a traditional view, this represents the need to overlap the π-systems of ethene and butadiene. This angle of attack is seen clearly in the upper of the two stereoviews shown in Figure 4. In this context, the ethene–butadiene transition state stands in sharp contrast with the dioxinone transition state shown in Figure 2. As mentioned above, and as illustrated in the top stereodrawing in Figure 2, the plane of the acetone moiety is tilted at roughly 90° relative to the plane of the acylketene. This approach does not allow for the orbital overlap traditionally described for the Diels–Alder transition state. Replacing the Diels–Alder type overlap is the overlap with the ketene LUMO. In butadiene, both the HOMO and LUMO lie above and below the plane of the molecule and thus dictate that the best overlap with this system and ethene will be from directly above or below the plane of butadiene. In acylketene, however, the HOMO lies above and below the plane of the molecule, but the LUMO has a large expression in the plane of the molecule.[20] This expression is particularly prominent at the αC of the ketene (C2). This observation explains why we see the acetone carbonyl oxygen attacking nearly in the plane of the acylketene, as opposed to the roughly vertical attack in the Diels–Alder transition state (Figure 2 vs Figure 4). In a Diels–Alder transition state, one can draw an uninterrupted π-system forming σ-bonds, all using parallel p type orbitals. In the dioxinone transition state **5**, there are points where seemingly orthogonal π-systems must be simultaneously modified for the reaction to proceed. The electophilic/nucleophilic interaction of O9–C2 and O5–C6 and their relative orientations shown in Figure 2 suggest a directional influence of lone-pair electron interactions. The possibility that the Diels–Alder-oriented complex may have lain along the reaction coordinate earlier than transition state **5** was pursued with the AM1 Hamiltonian by following the intrinsic reaction coordinate (IRC) with Gaussian 92.[21] This showed only an extension of the breaking bonds with no radical changes in the orientational geometry. Due to distinct differences between the dioxinone transition

(20) This can be seen in solid orbital representations conducted using wave functions generated on Spartan software from AM1 calculations we have done on acylketene. This is also known in the literature for ketenes in general: (a) Houk, K. N.; Stozier, R. W.; Hall, J. A. *Tetrahedron Lett.* **1974**, 897. (b) Skancke, P. N. *J. Phys. Chem.* **1992**, *96*, 8065. Experimental evidence: (c) Tidwell, T. T. *J. Am. Chem. Soc.* **1987**, *109*, 2774.

state **5** and the prototypical Diels–Alder transition state shown in Figure 4, it might be best to refer to this system generically as a [4 + 2] retro-cycloadditon, rather than a retro-Diels–Alder reaction.

Though the discussion has thus far focused primarily on dioxinone system **1**, it should be pointed out that the contrasting observations relevant to dioxinone transition state **5** and the Diels–Alder transition state shown in Figure 4 hold true for oxazinone transition state **6** as well. The dioxinone transition state **5** and the oxazinone transition state **6** are quite similar.

Looking at the differences between the enthalpy of activation for the thermal cycloreversion of oxazinone **3** and dioxinone **1** in Table 4, it becomes evident that, at most levels of calculation, the enthalpy of activation for the thermal decomposition of oxazinone is in the vicinity of 15 kcal/mol higher than it is for dioxinone. In looking to the calculations for a qualitative guide to potential synthetic utility of oxazinone **3**, we must bear in mind the vagaries of our quantitative results. We have not performed a study demonstrating saturation of basis set or of correlation energy. Further, the role of the solvent in modifying activation energies is completely ignored. With these limitations in mind, we see that the AM1 and MP2/6-31G*//HF/3-21G (ZPE) calculations compare favorably both with each other and with the experimental solution phase enthalpy of activation for the thermal cycloreversion of dioxinone. We look to these calculations for oxazinone **3**. AM1 gives $\Delta H^{\ddagger} = 46.4$ kcal/mol, and MP2/6-31G*//HF/3-21G (ZPE) gives $\Delta H^{\ddagger} = 44.2$ kcal/mol. These results are also in good agreement with several other single-point calculations, and we regard them as our best estimate of the experimental enthalpy of activation for the thermal cycloreversion of oxazinone **3**.

To our knowledge, oxazinone **3** has not been synthesized, and therefore, its thermal stability is unknown. Other 4*H*-1,3-oxazin-4-ones, where the noncarbonyl oxygen and the nitrogen switch places, are thought to thermally decompose.[22] The predicted enthalpies of activation for the thermal cycloreversion of oxazinone suggest that oxazinone **3** would behave in a manner similar to that of dioxinone **1** but would require higher temperatures for the thermal decomposition to occur. Boeckman[2c] used mild acid catalysis ($PyH^+ {}^-OTs$) to produce a β-keto amide from a substituted dioxinone and glycene methyl ester in refluxing tetrahydrofuran. The boiling point of THF is 67 °C. This is well below the operational temperature of the uncatalyzed thermal cycloreversion of dioxinone, which is usually run in refluxing toluene (111 °C) or refluxing xylenes (137–144 °C). These facts suggest that, while oxazinone **3** has a higher activation barrier toward thermal decomposition than does dioxinone **1**, it could still be a viable synthetic reagent were it used with mild acid catalysis. Our lab is currently pursuing the synthesis of an analog of oxazinone **3** to determine its usefulness as a reagent in organic synthesis.

Conclusion

We have shown two interesting and unique transition states for a process that, on its face, looks to be a retro-Diels–Alder reaction, yet due to the attack angle of the acetone moiety relative to the plane of the acylketene moiety of dioxinone transition state **5**, we conclude that this process only remotely resembles a Diels–Alder transition state. Rather, it appears to be a nucleophilic attack by the acetone carbonyl oxygen at the ketene αC in concert with an electrophilic attack by the acetone carbonyl carbon on the acylketene carbonyl oxygen, O5. This gives a transition state appearing Diels–Alder-like on the written page but quite unlike a Diels–Alder transition state as a three-dimensional model. Additionally, we have given qualitative energetic data which suggest that the thermal cycloreversion of oxazinone **3** would require more energy and consequently higher reaction temperatures than those required for the thermal decomposition of dioxinone **1**.

Acknowledgment. We are grateful to the National Science Foundation (Grant CHE 9406891) and Research Corp. (Cottrell Research Grant 9477) for financial support of this research. We also thank the reviewers for their many helpful suggestions.

Supplementary Material Available: Cartesian coordinates for the HF/3-21G-optimized structures, vibrational analyses, and Mulliken bond order and charge analysis (83 pages). This material is contained in libraries on microfiche, immediately follows this article in the microfilm version of the journal, and can be ordered from the ACS; see any current masthead page for ordering information.

JO950460O

(21) Frisch, M. J.; Trucks, G. W.; Head-Gordon, M.; Gill, P. M. W.; Wong, M. W.; Foresman, J. B.; Jonson, B. G.; Schlegel, H. B.; Roff, M. A.; Replogle, E. S.; Gomperts, R.; Andres, J. L.; Raghavachari, K.; Binkley, J. S.; Gonzalez, C.; Martin, R. L.; Fox, D. J.; Defrees, D. J.; Barker, J.; Sewart, J. J. P.; Pople, J. A. *Gaussian 92*, Revision A; Gaussian, Inc.: Pittsburgh, PA, 1992.

(22) Sato, M.; Ogasawara, H.; Yoshizumi, E.; Kato, T. *Chem. Pharm. Bull.* **1983**, *31*, 1902.